Celal Bayar University Journal of Science

Impact of Thickness and Composition on YAG:Ce Composite Scintillators for Alpha Particle Detectors

Onur Buğra Kolcu[1]*

[1] Istinye University, TR-34010, Istanbul, Türkiye
* onur.kolcu@istinye.edu.tr
* Orcid No: 0000-0002-9177-1286

Received: December 10, 2024
Accepted: April 7, 2025
DOI: 10.18466/cbayarfbe.1599240

Abstract

This study evaluates the performance of imaging-based alpha particle detectors using YAG:Ce composite scintillators in mixed radiation fields. Scintillators with varying thicknesses (0.1 mm, 0.5 mm, and 1.0 mm) and YAG:Ce to epoxy ratios (5%, 15%, and 20%) were modeled using the GEANT4 simulation package to analyze the detection efficiency, light output, and energy resolution of the alpha particle detectors. The results indicate that a 0.5 mm thick scintillator with 90% YAG:Ce and 10% epoxy is the optimal configuration among the simulated scintillators for an alpha particle detector. Additionally, phantom-based simulations demonstrated that the detector is capable of producing clear imaging of alpha particles.

Keywords: *YAG:Ce scintillator, Alpha particle detectors, GEANT4, Simulation*.

1. Introduction

Alpha particle detectors are widely used in various fields, including monitoring natural radioactivity, nuclear physics, space research, and radiation safety [1-3]. Their applications have expanded into the medical field as well, due to the growing use of alpha-emitting isotopes in medical treatments [4, 5]. Moreover, following the devastating earthquake in Japan that hit the Fukushima Daiichi Nuclear Power Plant (FDNPP), alpha particle detectors were employed to assess contamination caused by radioactive substances such as ^{238}Pu and ^{239}Pu. This disaster underscored the need for advanced detection methods and led to increased research into imaging-based alpha particle detectors [6-8].

Currently, ZnS(Ag) scintillation detectors are commonly used for the detection of alpha particles [9-13]. However, due to its opacity and limited energy resolution, there are challenges in identifying alpha-emitting radioisotopes or distinguishing natural radiation caused by Radon (Rn) from radiation originating from nuclear fuels [14, 15]. A potential solution to these limitations is to use alternative scintillators that offer good energy resolution and enhance the ability to utilize two-dimensional distribution differences to distinguish Plutonium (Pu) from Radon (Rn) progeny, such as ^{214}Po and ^{218}Po [16, 17]. Therefore, there is growing interest in developing imaging-based alpha particle detectors using scintillators capable of providing good energy resolution and spatial resolution.

In line with this trend, several recent studies have focused on improving scintillation-based alpha particle detectors. For instance, an alpha particle imaging detector was developed to assess nuclear contamination at the Fukushima Daiichi Nuclear Power Plant (FDNPP) by coupling a 0.05 mm-thick $Gd_3(Ga,Al)_5O_{12}$ (GAGG:Ce) scintillator to a 1 mm-thick glass plate and a 1 mm-thick acrylic light guide, with signal readout achieved using an 8 × 8 silicon photomultiplier (SiPM) array [17]. Analysis of smear papers collected from the FDNPP site confirmed that alpha emitters within the reactor buildings originated from nuclear fuels. Additionally, it was reported that this finding could not have been obtained using ZnS(Ag) detectors [17]. Similarly, Yamamoto et al. utilized a 1 mm-thick GAGG:Ce scintillator coupled to a 1 mm-thick light guide and an 8 × 8 SiPM array, employing pulse shape discrimination to distinguish alpha signals from gamma signals, resulting in high-resolution alpha imaging [18]. Additional approaches have included coupling a 1 mm-thick $YAlO_3$:Ce (YAP:Ce) scintillator to a photomultiplier tube (PMT), as demonstrated by Unzueta et al., resulting in sub-millimeter position resolution for alpha detection [19]. Yasuda et al. utilized a phoswich detector composed of ZnS(Ag) powder, YAP:Ce, and $Y_3Al_5O_{12}$:Ce (YAG:Ce) scintillators to simultaneously measure alpha and

beta/gamma emissions [20]. Shimaoka et al. further explored $Gd_2Si_2O_7$ (GPS) scintillator powders applied at a 0.1 mm equivalent thickness onto 1 mm-thick glass substrates and coupled to a PMT, determining the optimal grain size for alpha particle detection [21].

Due to their short range, alpha particles can be detected using scintillators such as GAGG:Ce, YAP:Ce, and YAG:Ce, which can be manufactured as thin screens, and studies involving these materials, as described above, have been extensively reported in the literature. Most studies focus on alpha particle detectors constructed from scintillators of similar thickness produced via growth methods or from composite scintillators. Research involving composite scintillators has been focused on determining the optimal particle size to achieve maximum light output and energy resolution [20-22]. However, investigations into changes in detector response due to variations in the concentration of binder material used with scintillator powders for GAGG:Ce, YAP:Ce, and YAG:Ce are limited.

This study focuses on determining the appropriate thickness for an alpha particle detector constructed using a YAG:Ce composite scintillator and examines the effects of binder material concentration (specifically epoxy) on light output, energy resolution, and detection efficiency through GEANT4 simulations. The primary objective is to determine the optimal design for an imaging-based alpha particle detector suitable for applications in mixed radiation environments, such as nuclear power plants planned for construction in Turkey. Additionally, this work will serve as a feasibility study for future prototyping efforts.

2. Materials and Methods

2.1. Alpha Detector Module

The YAG:Ce scintillator, with its refractive index of 1.82, density of 4.57 g/cm³, non-hygroscopic property, light output at approximately 40% of that of NaI:Tl scintillators, emission wavelength around 530 nm, and ability to provide relatively good energy resolution, is a suitable scintillator for nuclear spectroscopy applications [23, 24]. Its dual-component decay times of 88 ns and 300 ns make it well-suited for pulse shape discrimination to distinguish alpha and gamma particles [25]. Furthermore, its high mechanical strength allows it to be fabricated into extremely thin structures, making it an ideal scintillator for use in alpha detectors in mixed radiation environments. Another advantage is that YAG:Ce single-crystal, ceramic and composite scintillators exhibit similar properties, offering flexibility in the production of scintillators with various geometries and thin structures [26].

In this study, the responses of alpha particle detectors constructed with YAG:Ce composite scintillators were investigated for thicknesses of 1 mm, 0.5 mm, and 0.1 mm. The scintillator width was set to 13 × 13 mm² to match the total width of the SiPM array, which was based on the Hamamatsu S13361-3050AE-04. In individual simulations for each scintillator thickness, the scintillators were coupled to a light guide made from 1 mm thick epoxy material. To detect the scintillation photons, a 4 × 4 SiPM array, with each SiPM having an area of 3 × 3 mm², was coupled to the light guide. The SiPM array was mounted on a printed circuit board (PCB) made of copper. To minimize photon leakage and optimize light collection efficiency, the scintillator and light guide were enclosed in an aluminum foil layer. The aluminum foil has a thickness of 3 µm on the front side of the scintillator and 0.5 mm on the lateral sides of the scintillator and light guide. The geometry used in the simulations is shown in Figure 1.

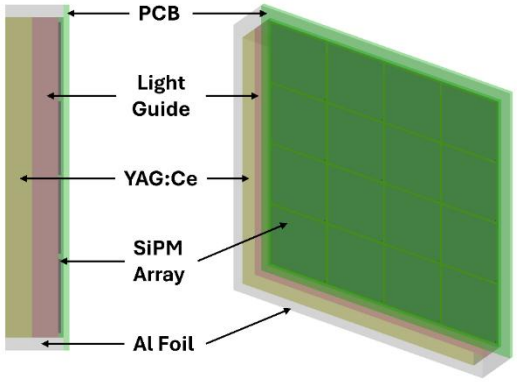

Figure 1. Lateral (left) and angled (right) views of the simulation geometry with a 1 mm thick YAG:Ce scintillator. The same setup was used for all YAG:Ce thicknesses.

For the material definition of the YAG:Ce scintillator in simulations, the volumetric mixing ratio of scintillator to epoxy was set at 90% and 10%, respectively, and the mixture's properties were assigned using weighted averages. The configuration yielding optimal light output and energy resolution for alpha particle interactions was selected by comparing the outputs obtained from three simulation setups with different thicknesses. Subsequently, the epoxy content was volumetrically varied (5%, 15%, 20%), and the resulting changes in detector response were analyzed.

2.2 Monte Carlo Simulations

The Monte Carlo simulations for the alpha particle detector were performed using the GEANT4 simulation package (version 11.1.2) [27]. GEANT4 is ideal for modeling particle interactions within matter and provides realistic outputs for the behavior of optical photons in materials. Therefore, this simulation package is highly suitable for examining the performance of a scintillation-based alpha particle detector.

Section 2.1 outlines the general structure of the detector and the assigned materials. The reflective surfaces of the aluminum foil, which enclosed the scintillator and light guide, were modeled using the GLISUR model. The surface finish was defined as "polished" with a dielectric-metal interface. The surface smoothness was set to 0.9 to simulate a slightly imperfect polished surface, creating a realistic interface between the scintillator and aluminum foil, as well as between the light guide and aluminum foil.

In the simulations performed for the alpha particle detector, radioactive sources ^{241}Am, ^{137}Cs, and ^{90}Sr were used. The ^{241}Am source was modeled as a monoenergetic point source with dominant gamma and alpha decay energies of 59.5 keV and 5.49 MeV, respectively. The alpha particles emitted from ^{241}Am are at energy levels similar to those emitted by radioactive elements such as ^{238}Pu (E_{alpha} ~ 5.49 MeV) and ^{239}Pu (E_{alpha} ~ 5.15 MeV) [28, 29]. Due to this similarity in alpha particle energies, only the ^{241}Am source was used in simulations to save computation time. Another reason for this choice is that the ^{241}Am source is readily available in our laboratory, allowing the planned prototype to be tested with this source in future experiments. To investigate the response of the alpha particle detector in a mixed radiation environment, other radioactive sources reported as contaminants at the FDNPP, such as ^{137}Cs and ^{90}Sr, were included in the simulations [17]. This allowed the evaluation of the detector's response to alpha, beta, and gamma particle interactions across various scintillator thicknesses and YAG:Ce/epoxy mixing ratios. The ^{137}Cs source was modeled as a monoenergetic gamma source, while ^{90}Sr was used as a predefined ion source in GEANT4. All radioactive sources were positioned at 2 mm from the detector, and 10^6 events within the detector's solid angle were generated for each source.

Optical photons produced by scintillation were transferred to the SiPM array via the light guide in the simulations. The SiPM array was modelled based on the dimensions and specifications of the Hamamatsu S13361-3050AE-04. This SiPM array was chosen for the simulations because its photon detection efficiency (40% at 450 nm with a spectral response range of 320 to 900 nm) aligns with the emission wavelength distribution of YAG:Ce [30]. Based on the number of detected optical photons, the light output, relative energy resolution, and detection efficiency of detectors modeled with different configurations were determined.

Since the energy resolution of the full energy peak of a scintillation-based detector is affected by various factors, such as the intrinsic resolution of the scintillator, transfer resolution, statistical contribution of the photodetector, and dark noise contribution, accurately determining the energy resolution using the GEANT4 simulation package is challenging [31, 32]. Therefore, instead of directly determining the energy resolution for the relevant energy peaks, the relative changes were analyzed to evaluate which detector configurations could offer relatively good energy resolution for an alpha particle detector.

3. Results and Discussion

The detection efficiency for alpha, beta, and gamma particles was evaluated using scintillators composed of 90% YAP:Ce and 10% epoxy at thicknesses of 0.1 mm, 0.5 mm, and 1 mm. The detection efficiencies presented in Table 1 were obtained based on the interaction of 10^6 particles within the detector's solid angle. As expected, the gamma detection rate of the detector increases with increasing scintillator thickness. This trend is evident from the rise in detection efficiency values observed for ^{137}Cs and ^{241}Am radioactive sources (see Table 1). Since the ^{241}Am source emits both gamma and alpha particles, its detection efficiency represents a combined efficiency. The energy difference between alpha and gamma particles emitted by the ^{241}Am source facilitates the separation of their corresponding peaks. However, taking advantage of the simulation environment, monoenergetic alpha particles with an energy of 5.49 MeV were generated, and the detection efficiency specifically for alpha particles emitted by ^{241}Am was also determined. As expected, the detection efficiency for alpha particles exceeded 99% across all scintillator thicknesses (see Table 1 – Det. Eff. (^{241}Am) (*)). Although the distance between the detector and the radioactive source was set to 2 mm, less than 1% of alpha interactions were observed outside the detector. This result may be due to the air used as the simulation medium or the coating on the front side of the scintillator. The interaction of beta particles emitted by the ^{90}Sr source increases with scintillator thickness, with a detection efficiency ranging between approximately 79% and 85%. The contribution of gamma rays emitted by the ^{137}Cs source to the alpha spectrum in a mixed radiation field was estimated to be at most ~10%.

Figure 2 shows the distribution of the detected number of optical photons using scintillators of three different thicknesses. This distribution can be interpreted as an uncalibrated energy spectrum, providing information about the light output as a function of scintillator thickness. As observed in Figure 2, the peak mean value corresponding to the alpha particles emitted by the ^{241}Am radioactive source increases as the thickness decreases. Additionally, the contribution of beta particles emitted by the ^{90}Sr radioactive source to the alpha peak region decreases with decreasing thickness. The overlap of beta spectra in the alpha peak region necessitates evaluating the background contribution from beta particles when determining the ideal configuration for the alpha particle detector. On the other hand, the ^{137}Cs spectra, obtained with scintillators of the assigned thicknesses, is distributed far from the alpha peak due to the limited

Celal Bayar University Journal of Science
Volume 21, Issue 3, 2025, p 72-79
Doi: 10.18466/cbayarfbe.1599240

Table 1. Detection efficiency (%) obtained for different particles emitted by ^{137}Cs, ^{90}Sr, and ^{241}Am radioactive sources as a function of scintillator thickness. Values marked with (*) represent the detection efficiency for alpha particles expected from the ^{241}Am source.

Scintillator Thickness	Det. Eff. (% - ^{137}Cs)	Det. Eff. (% - ^{90}Sr)	Det. Eff. (% - ^{241}Am)	Det. Eff. (% - ^{241}Am) (*)
0.1 mm	2.24	79.76	61.42	99.80
0.5 mm	6.17	82.11	84.26	99.96
1 mm	9.97	84.95	92.71	99.82

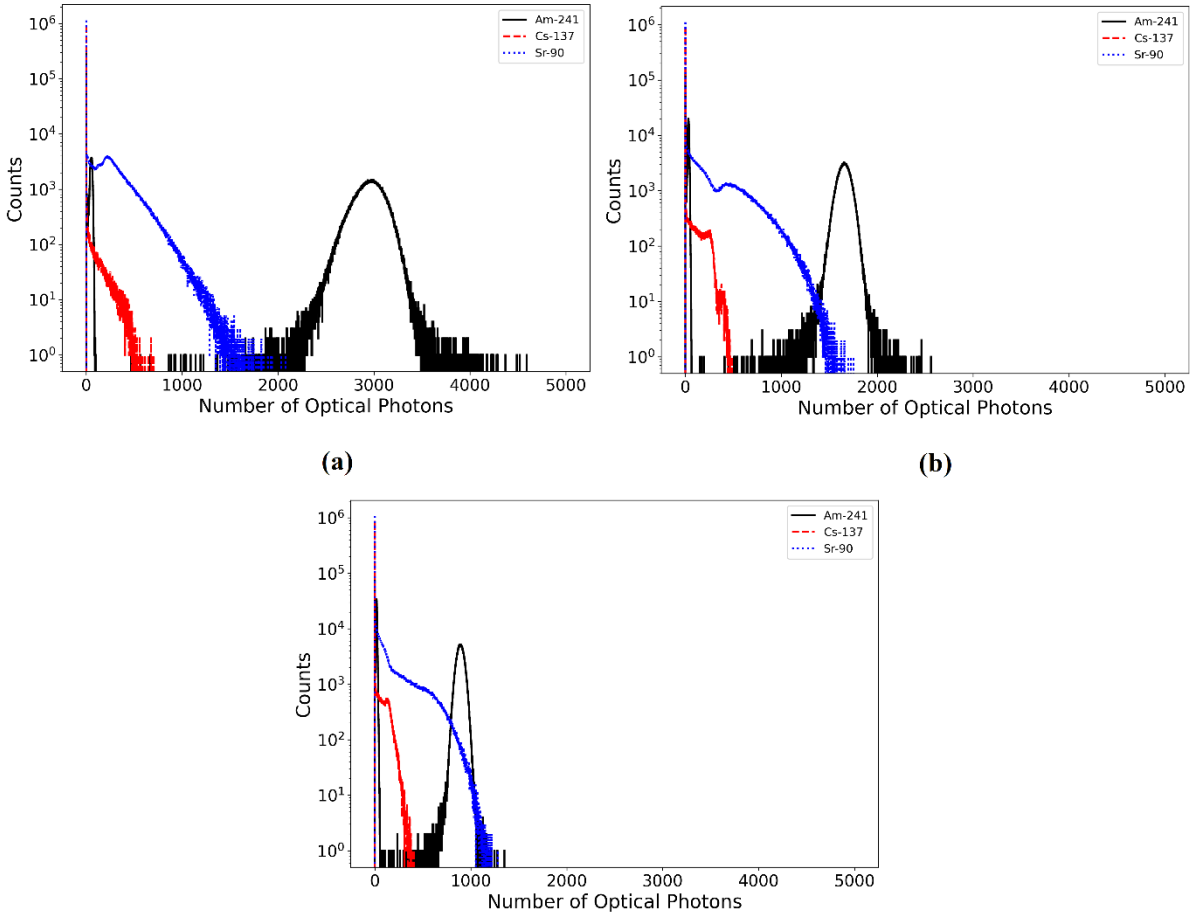

Figure 2. Distributions of the number of detected optical photons for different particle sources and scintillator thicknesses **(a)** 0.1 mm, **(b)** 0.5 mm, **(c)** 1 mm.

thickness of the scintillators and the relatively high energy of gamma rays. Therefore, for all scintillator thicknesses used in the simulations, the gamma rays from ^{137}Cs do not need to be considered as a potential background contribution.

To investigate the changes in light output and energy resolution with respect to scintillator thickness, the distributions provided for different radioactive sources in Figure 2 were summed, and the alpha particle peak was fitted with a Gaussian function within a 3σ range. Two data sets were generated from the combined distributions: the total spectra for ^{241}Am, ^{137}Cs, and ^{90}Sr, and the total spectra for ^{241}Am, ^{137}Cs (see Figure 3). The analysis of these two data sets was used to investigate the impact of beta-spectrum-induced background on energy resolution. This approach enables a more accurate determination of the detector's response in a mixed radiation field. From the fits applied to the alpha particle peak in the data sets, the light output (mean value of the peak) was found to be 2959.72 ± 0.39, 1655.56 ± 0.12, and 890.26 ± 0.11 for scintillator thicknesses of 0.1 mm, 0.5 mm, and 1 mm, respectively. The percentage increases in light output were calculated as

approximately 78.77% between 0.1 mm and 0.5 mm, 85.96% between 0.5 mm and 1.0 mm, and 232.46% between 0.1 mm and 1.0 mm.

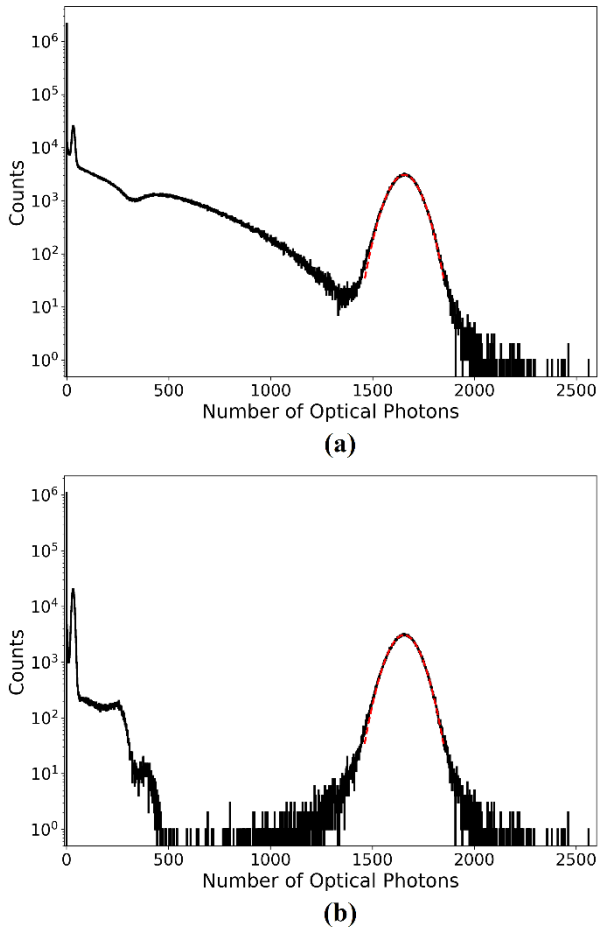

Figure 3. Total spectra for **(a)** ^{241}Am, ^{137}Cs, and ^{90}Sr **(b)** ^{241}Am and ^{137}Cs for a scintillator thickness of 0.5 mm. The dashed red line represents the fit curve within the 3σ region.

The same data sets were used to examine the relative change in energy resolution. To perform the analysis, the energy resolution obtained with a scintillator thickness of 0.1 mm was used as a reference, and the energy resolutions for different thicknesses were normalized to this value. In this way, the relative change in energy resolution was determined as a function of scintillator thickness.

In the ^{241}Am spectra corresponding to the 0.1 mm scintillator thickness (see Figure 2(a)), a partial asymmetry in the peak associated with alpha particles is observed. This asymmetry leads to the worst energy resolution being obtained from the data set with the 0.1 mm scintillator. The energy resolution improves by 18.76 ± 0.06% with the 0.5 mm scintillator and by 6.64 ± 0.03% with the 1.0 mm scintillator. When curve fitting was applied to the data set excluding the ^{90}Sr radioactive source, no change in energy resolution was observed for detectors using 0.1 mm and 0.5 mm scintillators. However, the energy resolution of the detector with the 1 mm scintillator improved by 9.20 ± 0.03%. This improvement can be attributed to the contribution of the beta spectrum in the peaking region, which, as seen in Figure 2(c), is most significant for the 1 mm scintillator.

Based on the results obtained for detection efficiency, light output, and energy resolution, the detector using a scintillator with a thickness of 0.5 mm yielded the most optimal results among the detectors used in the mixed radiation field. The 0.5 mm thick scintillator consisted of 90% YAG:Ce and 10% epoxy, which was taken as the reference and named YAG_{ref}. The response of the alpha particle detector was further investigated in terms of detection efficiency, light output, and relative energy resolution by varying the YAG:Ce concentration in the 0.5 mm thick scintillator to 5% (YAG-5/Ep-95), 15% (YAG-15/Ep-85), and 20% (YAG-20/Ep-80). Figure 4 presents the spectra for the four YAG:Ce concentrations investigated: YAG-5/Ep-95, YAG_{ref}, YAG-15/Ep-85, and YAG-20/Ep-80.

Changes in the YAG:Ce concentration do not significantly affect the spectral characteristics resulting from interactions with alpha, beta, and gamma particles, as shown in Figure 4. However, while detection efficiency for alpha particles remains unchanged (>99%), the detection efficiency for the ^{137}Cs radioactive source decreases as the epoxy content increases (from 6.37% for YAG-5/Ep-95 to 5.79% for YAG-20/Ep-80). An increase in epoxy content is expected to lead to a rise in Cherenkov events caused by beta particles. However, as seen in Figure 4, no significant change is observed in the spectral characteristics associated with beta interactions.

Using the detector with YAG_{ref} as a reference, the detector with YAG-5/Ep-95 demonstrated a 3.78% increase in light output, while detectors with YAG-15/Ep-85 and YAG-20/Ep-80 showed decreases of 3.89% and 7.93%, respectively.

To evaluate energy resolution across varying YAG:Ce concentrations, two data sets were analyzed: one incorporating all contributions (^{241}Am, ^{137}Cs, ^{90}Sr) and another excluding the ^{90}Sr contribution. No significant changes in energy resolution were observed in either case. While an improvement in energy resolution is expected with the increase in light output as YAG:Ce concentration rises, the observed improvement was minimal (0.65% improvement for YAG-5/Ep-95), and a slight degradation in energy resolution (0.33%) was observed for YAG-20/Ep-80. These findings suggest that increasing the epoxy ratio up to 20% in a scintillator constructed with YAG:Ce allows for the development of

Celal Bayar University Journal of Science
Volume 21, Issue 3, 2025, p 72-79
Doi: 10.18466/cbayarfbe.1599240

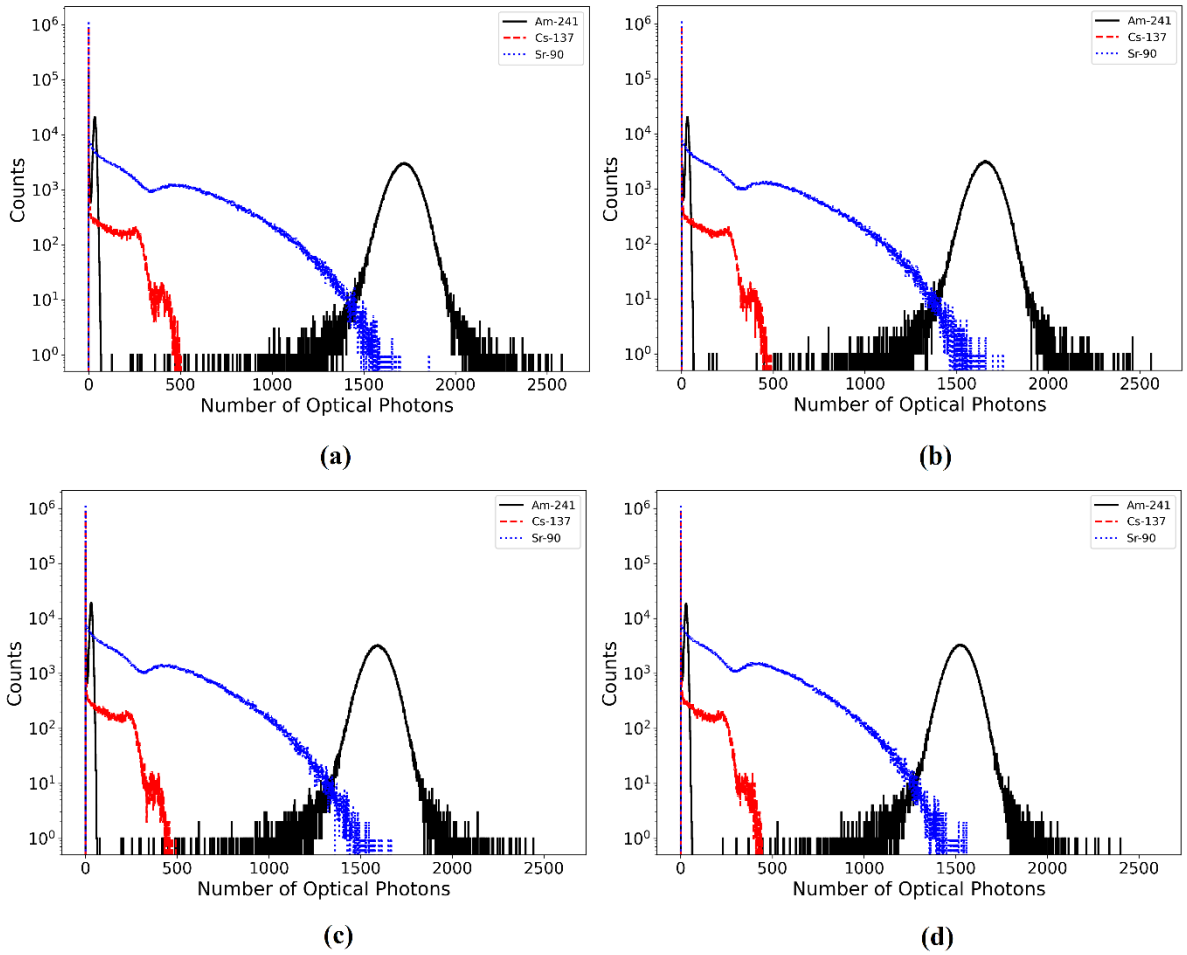

Figure 4. Distributions of the number of detected optical photons for different particle sources and YAG:Ce concentrations **(a)** YAG-5/Ep-95 **(b)** YAG_{ref} **(c)** YAG-15/Ep-85 **(d)** YAG-20/Ep-80. Plot **(b)** is identical to **Figure 2(b)** but presented on a different scale (0 to 2600) for easier comparison.

a more cost-effective detector without significant deterioration in energy resolution.

A potential imaging scenario for alpha particles was also investigated using the detector with the YAG_{ref} scintillator. Since the detector employs an SiPM array, it is possible to generate images using the center of gravity (COG) method [33]. To examine the capability, a 1 mm thick phantom with the same dimensions as the detector was utilized. The phantom included 12 horizontal gaps, each 0.1 mm wide, on its left side, and 6 vertical gaps, each 0.2 mm wide, on its right side. A simulation image of the detector with the phantom is shown in Figure 5. The ^{241}Am radioactive source was placed 2 mm away from the detector, configured to randomly distribute particles across the detector's front surface, and used to generate a total of 10^8 events.

To generate and enhance the image of alpha particles, background contributions from gamma rays emitted by the ^{241}Am radioactive source were excluded from the analysis under the condition number of optical photons bigger than 250. As shown in Figure 4, this roughly chosen threshold is sufficient to exclude 59.5 keV gamma rays from the analysis.

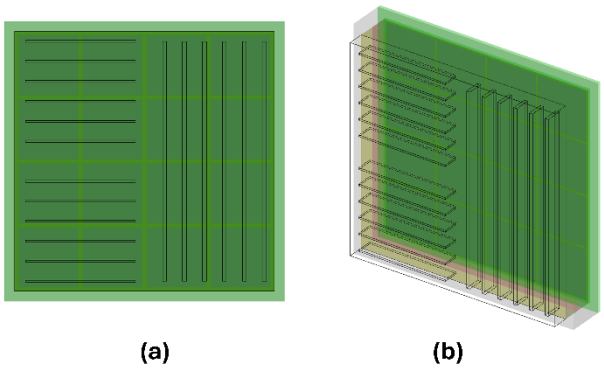

Figure 5. Front **(a)** and side **(b)** views of the phantom positioned on the detector's front face. The phantom is rendered transparent to highlight the vertical and horizontal gaps.

The COG method calculates the interaction point by weighting the physical positions of the SiPMs with the

number of photons they detect, effectively determining the centroid of the light distribution. The formulas for calculating the COG in the x and y directions are:

$$X = \frac{\sum_i (N_i \cdot x_i)}{\sum_i N_i}, Y = \frac{\sum_i (N_i \cdot y_i)}{\sum_i N_i} \quad \textbf{(3.1)}$$

where N_i represents the number of photons detected by the *i-th* SiPM, x_i, y_i are physical coordinates of the *i-th* SiPM, and $\sum_i N_i$ is the total number of photons detected across all SiPMs [33]. Figure 6 shows the image obtained from the simulation using the phantom. The image is relatively clear, and all gaps in the phantom are visible. However, shifts in the lines are present due to the pincushion effect, commonly observed in scintillator-based imaging detectors. This effect is expected when using the basic COG method, and methods to reduce the pincushion effect are well-documented in the literature. Since image enhancement is not the focus of this study, efforts to improve the images will be conducted in future work using data obtained from the physically constructed detector prototype planned for development.

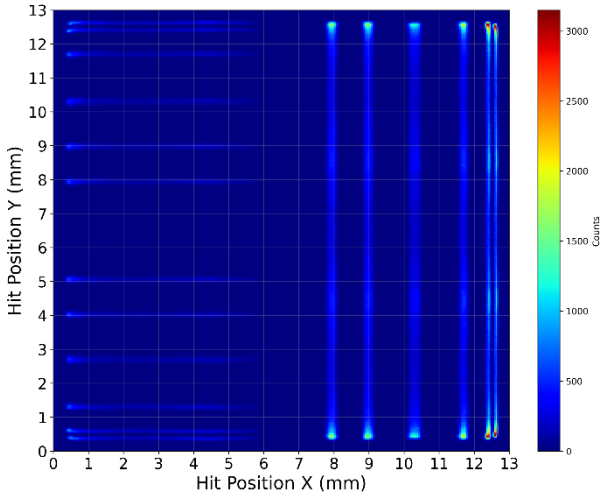

Figure 6. Heatmap of the phantom image illustrating the distribution of hit positions across the 13 mm × 13 mm SiPM array, with intensity indicating photon counts.

4. Conclusion

In this study, the optimal scintillator thickness and corresponding detector response for an imaging-based alpha particle detector suitable for use in a mixed radiation field were investigated using YAG:Ce scintillators of varying thicknesses. Additionally, the effects of changing the epoxy and YAG:Ce ratio in a scintillator on detection efficiency, light output, and energy resolution were examined.

Simulation results demonstrated that a detector constructed with a 0.5 mm thick scintillator provided the most optimal results in terms of detection efficiency, light output, and energy resolution. While an increase in light output was observed with changes in YAG:Ce concentration, no significant change in energy resolution was observed. This finding indicates that a more economical scintillator with 20% YAG:Ce and 80% epoxy content can also be used effectively as an alpha particle detector.

As a continuation of this simulation study, future efforts will focus on fabricating composite scintillators with YAG:Ce powders and developing an alpha particle detector. This will enable a direct comparison of parameters such as detection efficiency, light output, and energy resolution determined through simulations with experimental measurements. Experimental results will also allow the incorporation of corrections into the simulation environment, considering factors that are expected to influence energy resolution, such as afterpulses, dark counts, crosstalk of the SiPM detector, and noise contributions from the experimental setup. These corrections will enable more accurate determination of energy resolution and allow the study to be extended to investigate different thicknesses and concentrations.

Author's Contributions

Onur Buğra Kolcu: Conceptualization, methodology, analysis and investigation, drafting and writing the manuscript, performing the simulations and data analysis.

Ethics

There are no ethical issues after the publication of this manuscript.

References

[1]. Gam, DY, Lee, CY, Park, JY, Kim, H, Lim, JM. 2023. Study on the characteristics of airborne gross alpha and gross beta activities in the vicinity of nuclear facilities. *Nuclear Engineering and Technology*; 55(12): 4554–4560.

[2]. Feldman, WC, et al. 2004. Gamma-Ray, Neutron, and Alpha-Particle Spectrometers for the Lunar Prospector mission. *Journal of Geophysical Research Atmospheres*; 109(E7).

[3]. National Academies Press (US). 1999. Natural Radioactivity and Radiation. Evaluation of Guidelines for Exposures to Technologically Enhanced Naturally Occurring Radioactive Materials. https://www.ncbi.nlm.nih.gov/books/NBK230654/ (accessed at 01.12.2024).

[4]. Lassmann, M, Eberlein, U. 2018. Targeted alpha-particle therapy: imaging, dosimetry, and radiation protection. *Annals of the ICRP*; 47(3–4): 187–195.

[5]. Darwish, RA, Staudacher, AH, Bezak, E, Brown, MP. 2015. Autoradiography Imaging in Targeted Alpha Therapy with Timepix Detector. *Computational and Mathematical Methods in Medicine*; 2015: 1–7.

[6]. Morishita, Y, et al. 2021. Plutonium dioxide particle imaging using a high-resolution alpha imager for radiation protection. *Scientific Reports*; 11(1).

[7]. Morishita, Y, Hoshi, K, Torii, T. 2020. Evaluation of an ultra-thin plastic scintillator to detect alpha and beta particle contamination. *Nuclear Instruments and Methods in Physics Research Section A Accelerators Spectrometers Detectors and Associated Equipment*; 966: 163795.

[8]. Yamamoto, S, Tomita, H. 2018. Development of a high-resolution alpha-particle imaging system for detection of plutonium particles from the Fukushima Daiichi nuclear power plant. *Radiation Measurements*; 115: 13–19.

[9]. McElhaney, SA, Ramsey, JA, Bauer, ML, Chiles, MM. 1990. A ruggedized ZnS(Ag)/epoxy alpha scintillation detector. *Nuclear Instruments and Methods in Physics Research Section A Accelerators Spectrometers Detectors and Associated Equipment*; 299(1–3): 111–114.

[10]. Kim, H, Park, K, Han, B, Choi, KD, Cho, G, Chang, H. 2020. Study on ZnS(Ag) for alpha spectrometer using silicon-based photo sensor. *Journal of Instrumentation*; 15(10): P10020.

[11]. Tu, D., et al. 2024. Glass-ZnS: Ag scintillating composite for radiation detection. *Journal of the American Ceramic Society*, *107*(8), 5265-5273.

[12]. Marin, V. N., Trunov, D. N., Litvin, V. S., Sadykov, R. A., & Altynbaev, E. V. 2024. Read-Out System for Thermal Neutron Detectors Based on ZnS (Ag)/LiF Scintillator. *Journal of Surface Investigation: X-ray, Synchrotron and Neutron Techniques*, *18*(4), 894-899.

[13]. Zada, I. C., Osovizky, A., & Orion, I. 2024. Enhanced high-sensitivity multi-layer neutron detector based on LiF: ZnS (Ag) scintillator. *Scientific Reports*, *14*(1), 31446.

[14]. Kubota, N, Katagiri, M, Kamijo, K, Nanto, H. 2004. Evaluation of ZnS-family phosphors for neutron detectors using photon counting method. *Nuclear Instruments and Methods in Physics Research Section A Accelerators Spectrometers Detectors and Associated Equipment*; 529(1–3): 321–324.

[15]. Morishita, Y, et al. 2014. Performance comparison of scintillators for alpha particle detectors. *Nuclear Instruments and Methods in Physics Research Section A Accelerators Spectrometers Detectors and Associated Equipment*; 764: 383–386.

[16]. Iida, T, et al. 1983. An alpha-particle imaging system for detecting plutonium contamination. *Nuclear Instruments and Methods in Physics Research*; 212(1–3): 413–418.

[17]. Morishita, Y, Torii, T, Usami, H, Kikuchi, H, Utsugi, W, Takahira, S. 2019. Detection of alpha particle emitters originating from nuclear fuel inside reactor building of Fukushima Daiichi Nuclear Power Plant. *Scientific Reports*; 9(1).

[18]. Yamamoto, S, Kataoka, J. 2024. Development of an ultrahigh resolution 1 mm Si-PM array based GGAG alpha particle imaging detector with gamma or X-ray separation capability. *Nuclear Instruments and Methods in Physics Research Section A Accelerators Spectrometers Detectors and Associated Equipment*; 1066: 169623.

[19]. Unzueta, MA, Mixter, W, Croft, Z, Joseph, J, Ludewigt, B, Persaud, A. 2019. Position sensitive alpha detector for an associated particle imaging system. *AIP Conference Proceedings*.

[20]. Yasuda, K, Usuda, S, Gunji, H. 2000. Properties of a YAP powder scintillator as alpha-ray detector. *Applied Radiation and Isotopes*; 52(3): 365–368.

[21]. Shimaoka, T, Kaneko, JH, Izaki, K, Tsubota, Y, Higuchi, M, Nishiyama, S. 2013. Development of scintillator plates with high energy resolution for alpha particles made of GPS scintillator grains. *Nuclear Instruments and Methods in Physics Research Section A Accelerators Spectrometers Detectors and Associated Equipment*; 735: 110–114.

[22]. Korotcenkov, G, Ivanov, M. 2023. ZnS-Based Neutron and Alpha Radiation Detectors. Springer eBooks; 75–108.

[23]. Moszyński, M, Ludziejewski, T, Wolski, D, Klamra, W, Norlin, LO. 1994. Properties of the YAG:Ce scintillator. *Nuclear Instruments and Methods in Physics Research Section A Accelerators Spectrometers Detectors and Associated Equipment*; 345(3): 461–467.

[24]. Yanagida, T, et al. 2005. Evaluation of properties of YAG (Ce) ceramic scintillators. *IEEE Transactions on Nuclear Science*; 52(5): 1836–1841.

[25]. Ludziejewski, T, Moszyński, M, Kapusta, M, Wolski, D, Klamra, W, Moszyńska, K. 1997. Investigation of some scintillation properties of YAG:Ce crystals. *Nuclear Instruments and Methods in Physics Research Section A Accelerators Spectrometers Detectors and Associated Equipment*; 398(2–3): 287–294.

[26]. Mihóková, E, Nikl, M, Mareš, JA, Beitlerova, A, Vedda, A, Nejezchleb, K, D'Ambrosio, C. 2007. Luminescence and scintillation properties of YAG:Ce single crystal and optical ceramics. *Journal of Luminescence*; 126(1): 77–80.

[27]. Agostinelli, S, et al. 2003. Geant4—a simulation toolkit. *Nuclear Instruments and Methods in Physics Research Section A Accelerators Spectrometers Detectors and Associated Equipment*; 506(3): 250–303.

[28]. Asaro, F, Perlman, I. 1954. The Alpha- and Gamma-Ray Spectra of Pu238. *Physical Review*; 94(2): 381–385.

[29]. Asaro, F, Perlman, I. 1952. The Alpha-Spectra of Pu239 and Pu240. *Physical Review*; 88(4): 828–831.

[30]. Hamamatsu Photonics. MPPC array S13361-3050AE-04. https://www.hamamatsu.com/us/en/product/optical-sensors/mppc/mppc_mppc-array/S13361-3050AE-04.html (accessed at 30.11.2024).

[31]. Moszyński, M. 2003. Inorganic scintillation detectors in γ-ray spectrometry. *Nuclear Instruments and Methods in Physics Research Section A Accelerators Spectrometers Detectors and Associated Equipment*; 505(1–2): 101–110.

[32]. Moszyński, M, et al. 2015. Energy resolution of scintillation detectors. *Nuclear Instruments and Methods in Physics Research Section A Accelerators Spectrometers Detectors and Associated Equipment*; 805: 25–35.

[33]. Llosa, G, et al. 2009. Energy, Timing and Position Resolution Studies With 16-Pixel Silicon Photomultiplier Matrices for Small Animal PET. *IEEE Transactions on Nuclear Science*; 56(5): 2586–2593.